The interactions of 300 MEV negative PI-Mesons with complex Nuclei

P. G. J. T. Parkhouse

THE INTERACTIONS OF 300 MEV NEGATIVE PI-MESONS WITH COMPLEX NUCLEI

by

P.G.J.T. Parkhouse

Presented in candidature for the Degree of Master of Science

of the University of Durham

April, 1963

ABSTRACT

A stack of emulsion pellicles has been exposed to a 300 MeV beam of π^--mesons and their interactions with nuclei have been observed by following 140 m of track.

In order to analyse the events the usual techniques have been employed in addition to which a new method due to the author of measuring the ionization of tracks, steeply inclined to the emulsion plane, is presented.

The interaction lengths for the production of inelastic interactions and elastic scatterings are (37.9 ± 2.0)cm and (77.4 ± 5.8)cm respectively. An Optical Model analysis leads to an absorption coefficient and change in wave number of (1.5 ± 0.15) 10^{12} cm^{-1} and $-$~~(14.1 ± 1.4)~~ (1.32 ± 0.12) 10^{12} cm^{-1} respectively. The differences from the expected values are consistent with a reduction of the cross-section for elastic scattering within the nucleus of about 3 times.

The average energy for inelastically scattered pions varies with the angle of scattering and resembles that for the scattering of pions by free, stationary nucleons except that the energy in the forward direction is somewhat reduced. The angular distribution for the scattered pions shows near isotropy whereas the equivalent graph for scattering on free nucleons is strongly peaked in the forward direction.

A mode of interaction in which only a single collision of the pion with a nucleon occurs is proposed. The pion emerges without further collision and the struck nucleon goes on to make other collisions. The exclusion principle has been applied to an experimentally determined distribution of momentum in the nucleus and a strongly inhibitive effect results, producing an isotropic distribution of the secondary pions and a lowering of the average energy of these pions in the forward direction.

For absorption of the pion it is proposed that two absorbing nucleons are involved which go on to make other collisions.

Energy balances have been performed on the inelastic scatterings and absorptive events. They show good agreement with the available energy.

CONTENTS

PREFACE

The material in this thesis is an account of the work carried out by the author during 1959-1961 at Durham University. It is concerned with the elastic and inelastic interactions of 300 MeV π^--mesons observed in nuclear emulsion. Some of the results presented here have already been published (Finney et al. 1961).

In the experimental work on elastic scattering of the π^--meson, the author worked in collaboration with Mr. P.J. Finney and Dr. J.V. Major. The experimental work on the inelastic interactions has been the sole responsibility of the author.

The analysis of the work has been made jointly with Dr. Major.

LIST OF FIGURES

LIST OF TABLES

INTRODUCTION

Since high energy π-mesons have become available from accelerating machines it has been possible to study in detail the elementary interactions between the π-meson and the proton, and, to some extent, the neutron. The interaction schemes have been elucidated and the total and differential cross-sections for many of them have been determined.

To a much lesser extent the interactions of π-mesons with complex nuclei have been investigated. These may be elastic collisions in which the nucleus simply recoils or inelastic in which it disrupts. The general features of these may be understood in terms of the Optical Model. It is thought that the inelastic interaction takes place predominantly through collisions of the π-meson with single nucleons of the nucleus. That the meson does interact with groups of nucleons is shown by the process of absorption of the meson which requires two or more nucleons to be involved. After an initial collision with a nucleon, a meson may make further collisions in the nucleus before being absorbed or escaping from the nucleus.

The collision between the π-meson and a nucleon in the nucleus is expected to be similar to a collision with a free nucleon, though there are some modifications. These modifications are due firstly to the motion of the nucleons which alters

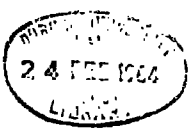

the energy available for interactions in the centre of mass system; secondly to the Pauli Exclusion Principle which must be applied to the nucleons which have been struck. Although the beam of π-mesons is mono-energetic the former effect leads to variations in the cross-section in the centre of mass system, though their average value is usually little different from that of the free nucleon cross-section at the energy of the π-meson beam. The second modification inhibits those collisions in which low values of momentum should be transferred to the struck nucleon and consequently this leads to a reduction of the cross-section.

It is possible to interpret the inelastic interactions of π-mesons with nuclei by taking into account these modifications to the free-nucleon cross-section as well as the possibility of interactions with groups of nucleons.

In addition to the inherent interest of the interactions of the π-meson with nuclei, a knowledge of the characteristics is essential to the understanding of the interactions of K-mesons or anti-protons with nuclei. In these interactions a π-meson is often the initial product of the interaction which is terminated by the interaction of the π-meson with the nucleus. These mesons are produced with energies of a few hundred MeV.

This laboratory has been investigating the characteristics of π-meson interactions with the nuclei of nuclear emulsions in the energy range 100 - 800 MeV. Blocks of emulsions have been exposed

to 88,300 and 750 MeV beams of π-mesons. The results of the elastic interactions at these energies have been published. In this thesis the elastic and the inelastic interactions of π^--mesons at 300 MeV are described.

In Chapter 1 the main features of the interactions of π-mesons with free nucleons are described briefly. The modifications to these are also considered. These are followed by a brief account of the Optical Model of interactions with the nucleus. This is used extensively in Chapter 3.

The complete analysis of the inelastic interactions has required the use of most of the identification techniques of nuclear emulsions. These are described in Chapter 2 where emphasis is given to the determination of ionization in steep tracks in the emulsion.

The details of the exposure, processing and scanning are given briefly in Chapter 3. The cross-sections for elastic and inelastic interactions are determined and the angular distribution of elastic scattering is given. These are analysed in terms of the Optical Model.

Chapter 4 presents the features of the inelastic interactions.

CHAPTER 1

THE INTERACTIONS OF π^--MESONS WITH NUCLEONS AND NUCLEI

The work described in this thesis is part of a programme on the investigation of the elastic and inelastic interactions of π^--mesons with complex nuclei of the nuclear emulsion between 100 and 800 MeV. The elastic interaction and the cross-sections for elastic and inelastic interactions are understood in terms of the diffraction and attenuation of a meson-wave by the nuclei of the emulsion. The former corresponds to the elastic interaction, the latter to the inelastic interaction. The understanding of the details of the inelastic interaction is made in terms of the collisions of the π-meson with individual nucleons of the nucleus. Moreover the degree of attenuation of the meson wave in the Optical Model is determined by this process. A summary of the main features of the collisions of pions with free nucleons is now given with the extent to which these collisions are modified when occurring in nuclei. This is followed by an account of the Optical Model.

1.1 Interactions of the π-meson with individual nucleons

The main interactions of charged mesons with nucleons in the energy range below 800 MeV are as follows:

1.1.1 $\pi^+ + p \rightarrow \pi^+ + p$

1.1.2 $\pi^+ + n \rightarrow \pi^+ + n$

} elastic scattering { $\pi^- + p \rightarrow \pi^- + p$; $\pi^- + n \rightarrow \pi^- + n$

1.1.3 $\pi^+ + n \rightarrow \pi^o + p$ charge exchange $\pi^- + p \rightarrow \pi^o + n$

1.1.4 $\pi^+ + n \rightarrow \gamma + p$ radiative capture $\pi^- + p \rightarrow \gamma + n$

The cross-sections for the first three equations are of the order of tens of millibarns but the cross-section for radiative absorption is of the order of 1 mb and so is negligible.

It should be noted that when elastic scattering occurs energy is transferred between the meson and the nucleon, both of which retain their initial identities.

Although the cross-sections for interaction with the neutron cannot be measured directly, it is expected by charge symmetry that the total cross-sections (σ_{π^+n}, σ_{π^-p}) should be equal as should be (σ_{π^-n}, σ_{π^+p}). The cross-sections σ_{π^+p} and σ_{π^-p} show a pronounced maximum at 190 MeV. At 300 MeV the values of the cross-sections are respectively 75 ± 5 mb and 32 ± 2 mb. The latter cross-section is made up of about 22 mb for elastic scattering and about 11 mb for charge exchange scattering; Yuan (1956).

Below 450 MeV the angular distribution for the scattered mesons has been investigated in detail. Above this energy the angular distributions are only partially known. In the centre of mass system the angular distribution is given by:

$$\frac{d\sigma}{d\Omega} = A + B \cos \theta^x + C \cos^2 \theta^x$$

where θ^x is the angle of scattering in the centre of mass system between the scattered π-meson and the incident one. The sign of B determines whether the distribution of scattering is predominantly forward or backward. Above 190 MeV this is positive (implying forward scattering) but below this energy backward scattering predominates for the elastic scattering of $\pi^{\pm}$-mesons. In figure 1 the angular distribution in the centre of mass system and the laboratory system are given for the elastic scattering of π^--mesons by protons and neutrons at 300 MeV.

1.2 Interactions with complex nuclei

A meson may interact with the whole of the nucleus elastically or with individual nucleons through processes 1.1.1 to 1.1.4. Although 1.1.1 and 1.1.2 are elastic collisions between the pion and the nucleon, the nucleus is left in an excited state because the nucleon has changed its energy. Hence all four interactions, 1.1.1 to 1.1.4, should be taken as inelastic interactions with the nucleus.

One or more nucleons may be knocked forward as a result of the interaction of the meson with individual nucleons; this leaves the struck nucleus in an unstable state. Equilibrium is subsequently attained, usually, by further nucleons being ejected. These nucleons are known as evaporation particles.

The π-nucleon cross-sections in the nucleus will be modified by the motion of the nucleons in the nucleus. For example, if a

Fig. 1A

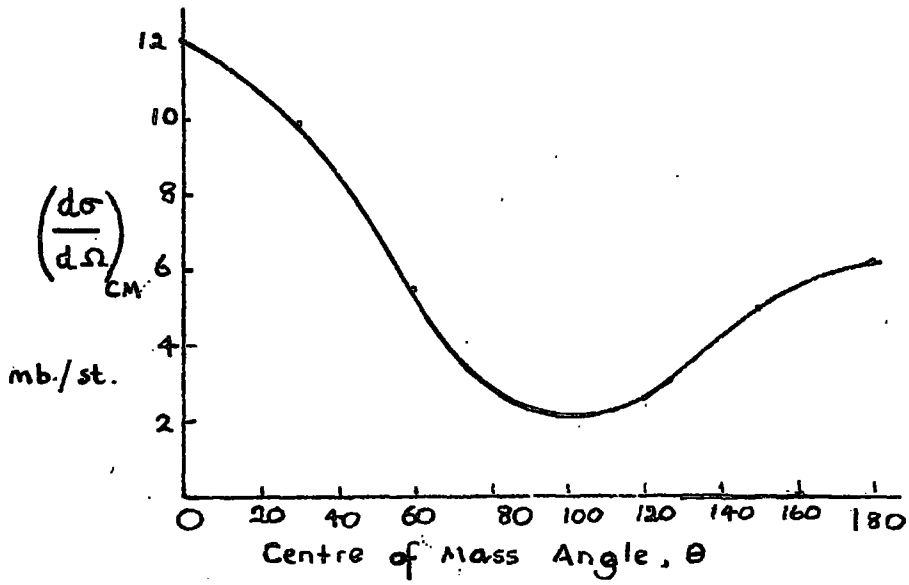

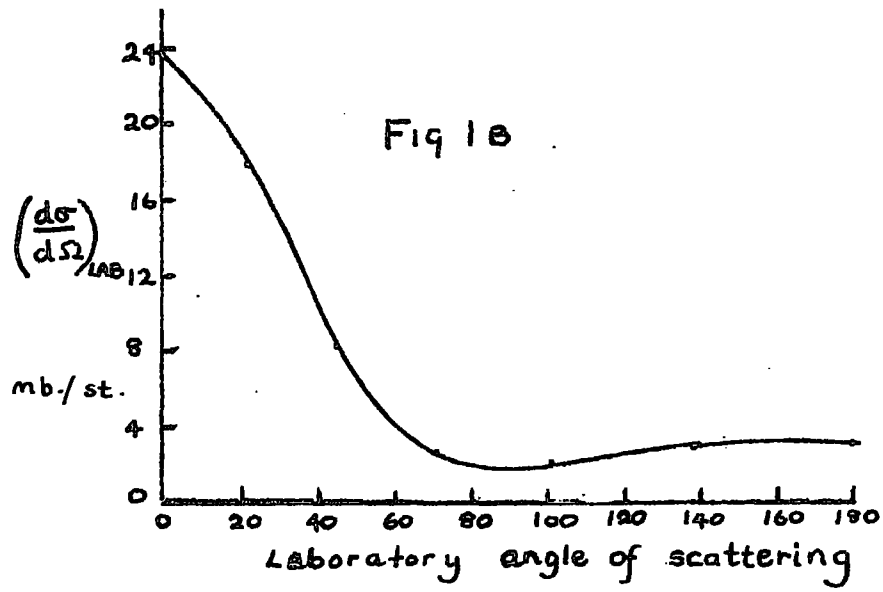

Fig 1B

The angular distribution for elastic scattering of π^--mesons by protons & neutrons, at 300 Mev.

300 MeV π^--meson collides with a proton moving towards it or directly away from it then the energy in the centre of mass will have values E_1 and E_2 from the two cases giving rise to two different cross-sections. For various possible angles of incidence between the meson and proton, there will be a continuous range of cross-sections for the interactions, bounded by the two values associated with E_1 and E_2. The mean cross-section, at 300 MeV, is slightly raised by this process.

A more important consequence of the motion of the nucleons is seen when the Pauli Exclusion Principle is applied. Any nucleon which has been struck is required to recoil with a momentum greater than some minimum value corresponding to the highest filled energy level of the nucleus. If the nucleon would have recoiled with a momentum less than the minimum then that collision is forbidden. These collisions correspond to the smaller angles of scattering of the π-meson. The expected effect is a reduction of the cross-section and a broadening of the angular distribution of scattering.

Finally the interactions in nuclei will be different from the π-nucleon case by the possibility of inelastic interactions with ~~one~~ two or more, nucleons. It is known that π-mesons are absorbed at rest in the nucleus chiefly by the following processes:

$$\pi^- + p + n \rightarrow n + n \qquad 1.2.1$$

$$\pi^+ + p + n \rightarrow p + p \qquad 1.2.2$$

It is expected that this process will be important even at energies different from zero.

The result of these modifications will be briefly stated. The π-meson-nucleon collision will be modified by the motion of the nucleons within the nucleus and by absorption by nucleon pairs.

The meson will therefore be scattered inelastically, scattered with charge exchange or be absorbed. The last two processes are difficult to separate unless the energy and identity of all the secondary particles are known. This is impossible to do, using the emulsion technique, since neutral particles leave no tracks. It is expected that, on average, nucleons emitted from absorption processes will carry away about 137 MeV more than in the case of charge exchange. If there is a known constant ratio, in all cases, between the total number and energy of emitted nucleons to charged nucleons emitted, it should theoretically be possible to distinguish between the two cases.

Suppose that the probabilities for absorption, charge exchange and inelastic scattering of π^--mesons by the nucleus are P_a, P_c and P_s then

$$P_a + P_c + P_s = 1 \qquad 1.2.3$$

The difference between the average total energy of the incident π-meson (W_π) and the average total energy received by all secondary nucleons [$\overline{E}_s = \Sigma$ (K.E.$_s$ + Binding Energy)] will be shared amongst

π-mesons undergoing charge exchange and elastic scattering.

$$W_\pi - \overline{E}_s = (P_c + P_s)(\overline{E}_\pi + m_\pi c^2) \qquad 1.2.4$$

The probability of scattering, P_s, is determined simply by identifying charged mesons in the secondaries to stars. There is uncertainty in the value of $\overline{E}_s$ because only the energy of the charged particles can be measured. The π^--meson interacts predominantly with neutrons than with protons and it is expected that a large part of the energy will be taken off by the neutrons.

1.3 The Optical Model of the nucleus

Serber (1947) pointed out that the nucleus will appear partially transparent to a high energy particle. This means that the mean free path in nuclear matter for such a particle is of the order of a nuclear diameter.

Fernbach, Serber and Taylor (1949) described a model of nuclear interaction in which a matter wave (the incident particle) is attenuated and diffracted by a nucleus which is treated as having both a refractive index and absorption coefficient. In the simplest case this refractive index is assumed constant throughout the nucleus.

The refractive index is related to the wave number of the incident meson outside the nucleus, k, and change in wave number k_1 as the wave enters the nucleus.

They show that the absorption cross-section will be given by

$$\sigma_a = \pi R^2 \left\{1 - [1 - (1 + 2KR)\exp(-2KR)]/2K^2R^2\right\} = f_1(K,R) \qquad 1.3.1$$

where R is the nucleus radius and K the absorption coefficient.

It is also shown that the diffraction scattering cross-section can be represented as

$$\sigma_d = f_2(K,R,k_1) \qquad 1.3.2 \qquad \text{(see Allen et al. 1959)}$$

$$= \pi R^2 \Big\{ 1 + [1 - (1 + 2KR)\exp(-2KR)]/2K^2R^2$$
$$- (1/(K^2/4 + k_1^2)^2R^2)[(K^2/4 - k_1^2) + \exp(-KR)$$
$$\times [2k_1R(K^2/4 + k_1^2) + k_1K] \sin 2k_1R - \exp(-KR)$$
$$\times [(K^2/4 - k_1^2) + KR(K^2/4 + k_1^2)] \cos 2k_1R\Big\}$$

The differential cross-section for diffraction scattering can be shown to be

$$\frac{d\sigma_d}{d\Omega} = \frac{\sigma_d}{\pi} [J_1(kR \sin\theta)]^2 [(1 + \cos\theta)/2]^2 \qquad 1.3.3$$

where J_1 is the first order Bessel function. It should be noted that the obliquity factor $[(1 + \cos\theta)/2]^2$ was not in the original paper by Fernbach, Serber and Taylor, but was suggested by Perkins and Fowler (1958).

The meson does not interact with the geometrical cross-section of the nucleus so one of two view points may be followed.

If there is an attractive force between the negatively charged meson and the positively charged nucleus, mesons will be drawn into

the nucleus, effectively increasing the absorption cross-section to σ_a'.

It can be assumed that $\sigma_a' = F \times \sigma_a$ where

$$F = 1 \pm \frac{2Ze^2E}{R(pc)^2} \qquad 1.3.4$$

Z = the nuclear charge, E = total energy of the meson whose momentum is ~~p~~ p.

The alternative viewpoint is due to Feshbach and Weisskopf (1949). Here the meson is supposed to have a characteristic "size" equal to the reduced de Broglie wavelength λ.

The new cross-section is σ_a'' given by

$$\sigma_a'' = (\sigma_a'^{1/2} + \pi^{1/2}\lambda)^2 \qquad 1.3.5$$

Similarly

$$\sigma_d'' = (\sigma_d'^{1/2} + \pi^{1/2}\lambda)^2 \qquad 1.3.6$$

At very low energies λ will be large and the correction will be important. Physically the size of the meson will be as large or larger than the geometrical cross-section of the nucleus and so the nucleus will then have lost all its transparency.

It is sometimes useful to consider the potential equivalent of the refractive index. This pictures the nucleus with a complex potential well with both real and imaginary parts, V_r and V_i. V_r introduces a phase difference between that part of the wave passing through the nucleus and that part not passing through the nucleus. Interference between these two wavefronts gives rise to diffraction. V_i is responsible for absorption of the wave in the nucleus and this

can enhance the diffraction effect.

Fowler and Perkins give

$$k - k_1 = k\,[1 + 2V_r/p\beta c + (V_r/pc)^2]^{\frac{1}{2}} \qquad 1.3.7$$

and $$V_i = \tfrac{1}{2}\,h\beta cK \qquad 1.3.8$$

where K is the absorption coefficient in nuclear matter.

K can be expressed as

$$K = \frac{A}{\frac{4}{3}\pi R^3}\,[\sigma_{\pi^- p}\,Z + \sigma_{\pi^- n}\,(A-Z)] \qquad 1.3.9$$

or by

$$K = \frac{N}{\frac{4}{3}\pi R^3}\,\sigma_D \qquad 1.3.10$$

when absorption by pairs of nucleons predominates. Here σ_D is the cross-section for absorption in deuterium and N is the effective number of deuterium pairs in the nucleus.

Also $$K = 1/\lambda_n \qquad 1.3.11$$

where λ_N is the mean free path in nuclear matter.

1.4 Application of the Optical Model to the emulsion

A value for the absorption coefficient, K, may be found by comparing the observed absorption cross-section with 1.3.1. The mean free path in nuclear matter then follows from 1.3.11.

The change in wave number, k_1, of the matter wave on entering the nucleus can be found from a comparison of the experimental angular distribution for diffraction scattering with the theoretical one 1.3.3. Most of the contamination, at 300 MeV, from scatterings in the coulomb field can be removed by neglecting any scattering with a projected angle of less than 5°.

By using the values for K and k_1 in the equations 1.3.7 and 1.3.8 the sizes of the real and imaginary parts of the optical potential can be found.

CHAPTER 2

TECHNIQUES OF IDENTIFICATION

The work on the inelastic interactions of π-mesons has required the identification of π-mesons amongst the secondary particles and the determination of the energies of all the secondary particles in order that an energy balance can be made. The former gives the probability of inelastic scattering whereas the lack of energy balance is used to distinguish between absorption and charge exchange of the primary meson.

The exposure was of 60 pellicles of emulsion. Tracks of particles could be traced from one pellicle to another allowing long lengths of track to be measured.

The characteristics which allow particles to be identified and their energies to be determined are range, ionization and scattering in the emulsion. The principles of the measurements of these quantities are now described.

2.1 Range

Very exact values of range were not required so the range was found by measuring the length of a track in each sheet of the emulsion. The length of the track in unprocessed emulsion is readily found if the shrinkage factor for each sheet is known. The identity of the particle was determined from the end characteristics of the

track: π^--mesons are recognised by δ-stars or in the absence of these by the characteristic scattering at the end of their range. If the track was not identified as a meson it was assumed to be that of a proton. This ignores the presence of α-particles in the secondary particles and leads to an underestimation of the energy carried away by charged secondaries.

The total range is converted into an initial kinetic energy using tables published by Fay et al. (1954). Graphs of range against energy have also been published by Powell et al. (1959).

The chief errors are in not being able to determine exactly where the track leaves the emulsion and the error in the track not being a straight line because of scatterings in the emulsion. The total error from these sources is estimated at 5%.

2.2 Track Density

In a developed track the number of grains per unit length is a measure of the ionization of the particle. The grains tend to coagulate to form groups or blobs. The density of blobs in a track can be found less subjectively than the grain density, which depends on the criteria adopted by observers as to the number of grains per blob. (Perkins and Daniells, 1954).

The blob density will depend on the degree of development of the emulsion; development variation can be corrected, to first order, by normalising the blob density against that of a standard

ionization in the emulsion. Such a standard is provided by the blob density of electrons which ionize at a constant value for energies in excess of about 5 MeV. Usually this is the method of normalisation. In the present work the exposure was deficient in electrons and so normalisation was made using the beam particles which ionize at a fixed value.

When a track is steeply inclined to the plane of the emulsion it is necessary to take a series of reference tracks throughout the depth of the emulsion. This is because the degree of ~~ionization~~ development varies quite considerably throughout the depth of the emulsion.

At high ionizations the blob density approaches zero as the track becomes totally clogged with grains. Between this state and that of minimum ionization, the normalised blob density passes through a maximum value of about 2.6. For tracks whose blob density is between zero and the maximum, the gap density is found, which, of course, equals the blob density. Here, the track has the appearance of very long blobs separated by gaps. It is useful to have this distinction in the measured quantities for discussion of ionization measurements.

Fig. 2a shows the experimental relationship between the number of blobs (or gaps) and grains in a track.

This curve was produced by counting the mean number of grains and blobs per standard length in flat tracks using a magnification (80 x 15 x 1.5). The blob outline enabled the number of grains in

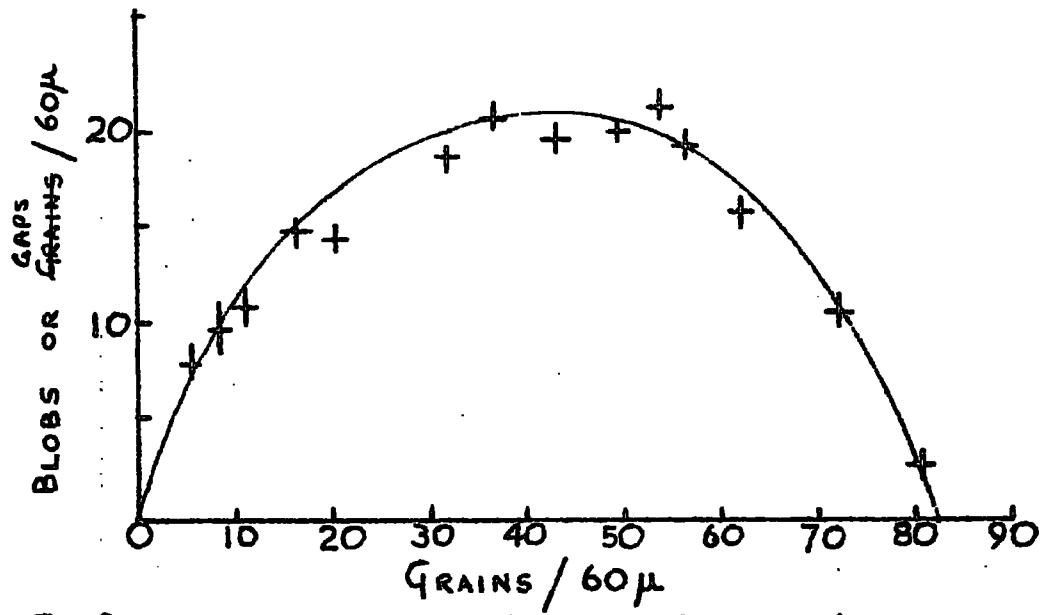

Fig 2A The variation between blobs and grains in a developed track.

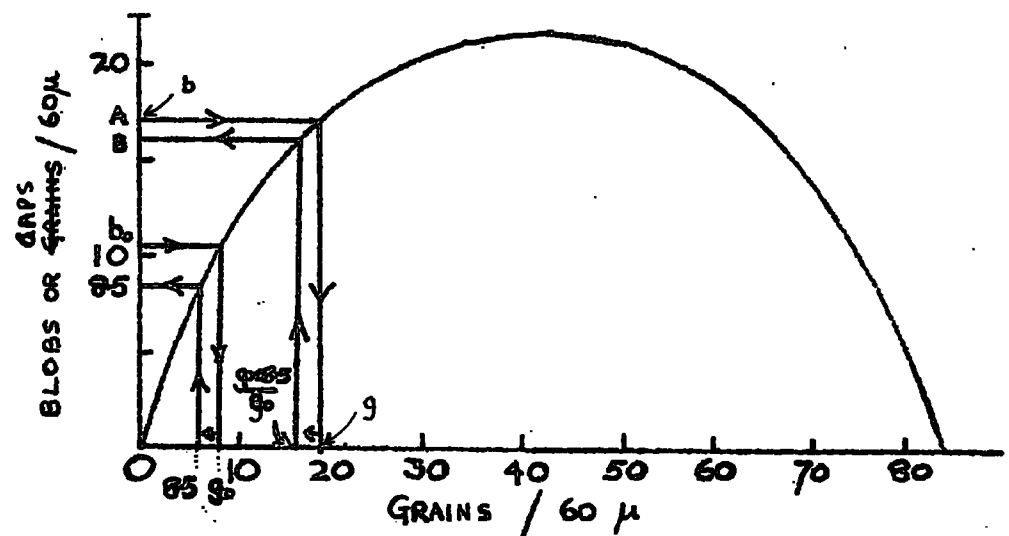

Fig 2B An example of the use of fig 2A in practice.

it to be found with little difficulty. The accuracy of this subjective test can be judged from the fact that the maximum number of grains to a cell of 60μ is 83, by extrapolation. This gives a grain diameter of 0.72μ, in good agreement with the measured diameter, using an eyepiece micrometer.

If a track were to pass through two regions of development, one of which caused twice as much development as the other, then the track should contain twice as many grains in one region as in the other region. Similarly the reference tracks would have twice as many grains in one region as in the other. By normalizing on grains the effect of development will be removed.

But normalising the blob density of the track which passes through the two different development regions will only partially remove the effect of development - i.e. this is the first order correction. The same track will appear to have two different ionizations in the two regions because the relationship between grain density and blob density is not linear. But by normalizing on a grain count this anomaly should be removed.

There are two reasons against such a practice. The first is that normalisation of a grain count gives a figure for the ionization (from 1 to 10) which is quite different from that obtained by the usual process of normalisation (from 1 to 2.3).

The second reason is that it would be tedious always to count the grain density of a track since it involves the estimation of grains in each blob. A compromise has been evolved.

The blob or gap density, b, is measured and fig. 2a is used to convert it into a grain density g. The standard blob density b_o is measured in the same region of development: this corresponds to a standard grain density g_o. If g_o is different from an arbitrarily chosen grain density of 8.5 grains/60μ, g_o and g are both adjusted proportionally until g_o is equal to the standard value and g is then g'. These values are then reconverted into b_o' (equal to 8.5 blobs/60μ) and b'. The normalised grain density is then $\bar{b}^x = \frac{b_o'}{8.5}$. This gives a good estimation of the ionization of a track in terms of numbers which are familiar. Fig. 2b shows, in diagramatic form, how the above is achieved.

An example of the correction will be given.

A track gave a blob count of 16 per 60μ in a region where that of the beam particle was 8.0 per 60μ. The simple, first approximation, normalisation gives a value of 2.00. Using the method advocated above a value for $\bar{b}^x = 1.95$ is found. If it is supposed that this track belongs to a proton then the energies corresponding to the two values of $\bar{b}^x = 2.00$ and $\bar{b}^x = 1.95$ are 390 MeV and 350 MeV respectively - a 16% variation in energy.

A correction for the inclination of the track in the emulsion must be made. This correction falls into two parts. The first part

is to correct the projected length of the track, as observed, into its true length. This naturally alters the blob density - the observed number of grains in a given projected length in the plane of the emulsion belong to a track length which is longer. The second correction is to remove the obscuring of gaps by grains in a track which is either steeply inclined or is less steeply inclined but which has a high blob density. In both cases the track appears blacker than it would if viewed normally.

In 1958 Viriasov and Pisareva, employing a suggestion made by Hodgson (1952), showed that the obscuring effect can be explained by introducing the concept of "dead-distance" analagous to "dead-time" in an electronic counting device. i.e. a grain is not seen separated from an adjacent grain by a gap if the grains are closer than some critical distance, the dead distance. For a flat track this dead distance is a grain diameter. Any two grains whose centres are closer than a diameter appear as a single blob.

According to Viriasov and Pisareva, the true number of grains in the track, N, is related to the observed number of blobs, n, by

$$N = \frac{n}{1-nd} \qquad 2.2.1$$

where d is the dead-distance. They also show that for an inclined track, any gap ℓ, where

$$\ell < 2r\ (\sec \beta - 1) \qquad 2.2.2$$

(the angle β is the angle between the track and the plane of the emulsion and r is the radius of the developed grain) is not seen - fig. 3.

The above formula, (2.2.1) may be applied in cases where the inclination, β, is not large and the grain density is low. It is not valid when these two conditions are not satisfied; this is because the formula uses a fixed dead distance (cp. fixed dead time).

In this work it has been necessary to identify particles of all degrees of steepness. This means that measurements have been taken on tracks which do not satisfy the criteria of Viriasov and Pisareva. It has been found that much better results were obtained using the following formula:

$$n = Ne^{-Nd} \qquad 2.2.3$$

Equation 2.2.1 is a first approximation of this equation. This formula, 2.2.3, uses a variable dead distance, d. But d is still given by $2r(\sec \beta - 1)$.

It should be noted that for a particular inclination of the track the dead distance is fixed. "Variable dead distance" is misleading but the term has been used because of its analogue "variable dead time".

It follows from the use of a variable dead distance that any number of successive grains in a steep track will be taken as a single blob if all the true gaps between the succession satisfy 2.2.2. This is what would be observed. Using 2.2.1, this same set of grains may well have given $N \nless 1$, which is not true.

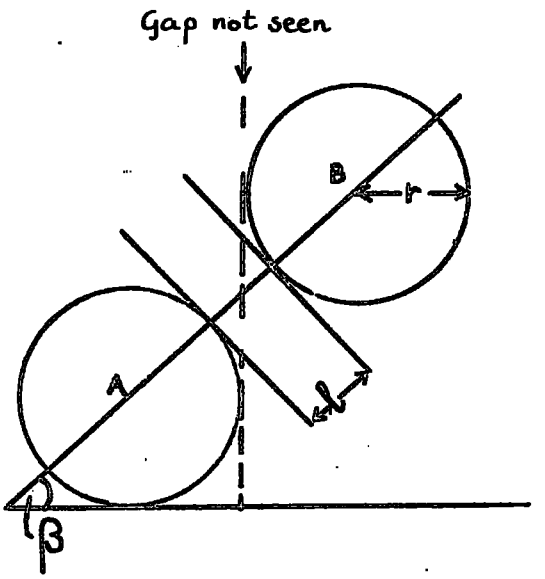

Fig 3 The obscuring of a gap by tilting the track.

The formula 2.2.3 has been tested experimentally. In the absence of tracks of known inclination, flat tracks have been used in the following way. The length of all the gaps in a set of tracks (which were flat) were measured using an eye-piece micrometer. An imaginary tilt was placed upon the track. This effectively chose a dead distance $d = 2r(\sec\beta - 1)$. In practice any gap less than this would not be seen. The number of blobs which would be seen at a given inclination is easily found from the observed gap distribution. Good agreement was found between the number given by the formula 2.2.3 and the number of blobs which would be seen for lightly ionizing tracks up to a pre-processed angle of dip of 65°. For tracks having an ionization of twice the minimum, it was necessary to take 2r as greater than 0.75μ which had been measured with the micrometer. A value of 1.00μ was found satisfactory.

As the ionization increased above $B^{x} = 2.00$ the effective diameter of the grain had to be gradually increased. This has been attributed to infectious development, which becomes more important as the grains become closer together.

A note on the application of the equation 2.2.3 in practice will be given. If it is re-written as $nd = Nde^{-Nd}$ 2.2.4 it can be easily plotted graphically as nd against Nd. Having found d, n is observed and so nd is known; from the graph Nd and hence N may be easily found.

This correction has been applied to all tracks. The result is that the observed blob densities can be explained in terms of dead distances and equation 2.2.4. The true blob densities can be therefore calculated.

The two corrections, one for the steepness of a track (which is in two parts) and the other for variable development have been applied to all measurements of B^x. In particular the results of the correction can be seen on the calibration curve showing the connexion between B^x and $p\beta$ for π-mesons. Fig. 4a shows uncorrected values for B^x against the corresponding $p\beta$ values for π^--mesons. Fig. 4b shows these same points which have been corrected. The continuous line represents the expected relation between the B^x and $p\beta$ values for flat π^--tracks. This continuous line has been drawn through the points of fig. 4b and also marked on 4a.

2.3 Scattering

When a charged particle passes through an emulsion it undergoes a large number of elastic scatterings in the electric fields of the atoms. The mean change in direction of the particle over a fixed distance is inversely proportional to the product, $p\beta$ for the particle.

The coordinate method of Fowler (1950) is used in which the mean angle of scattering $\overline{\alpha}_{100}$ over a cell length of 100μ is found. Then

$$p\beta = \frac{K}{\overline{\alpha}_{100}} \qquad 2.3.1$$

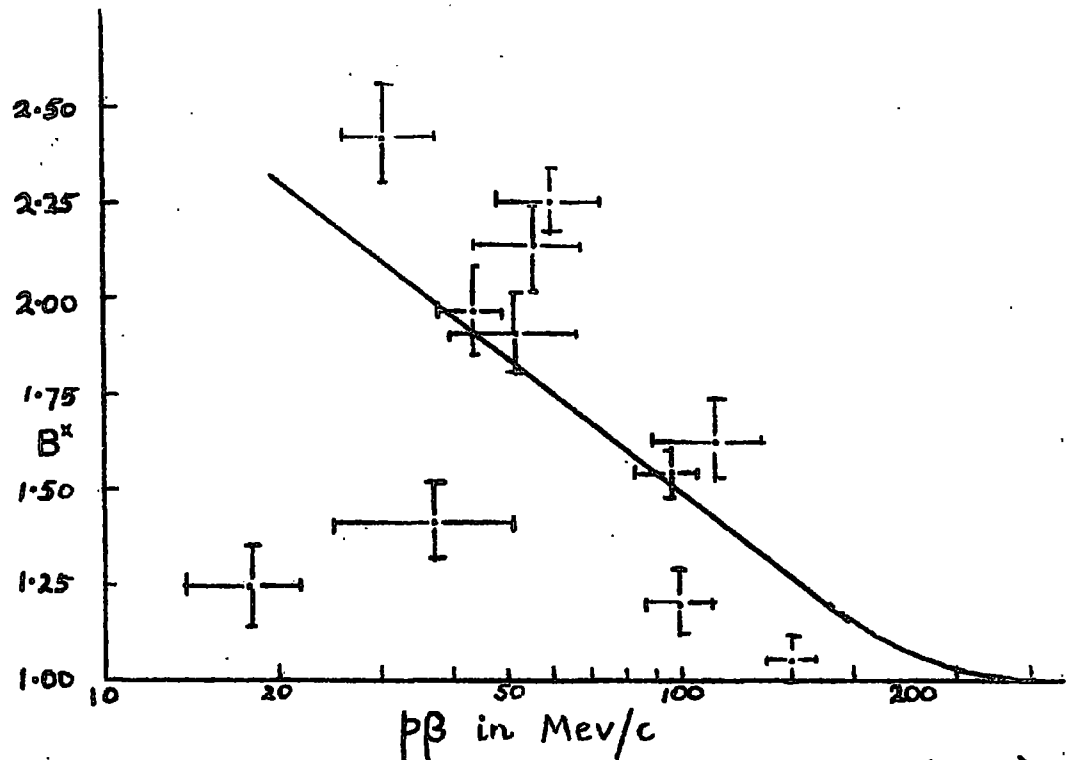

Fig 4A The relationship between uncorrected blob density and pβ for π^--mesons in G 5 emulsion.

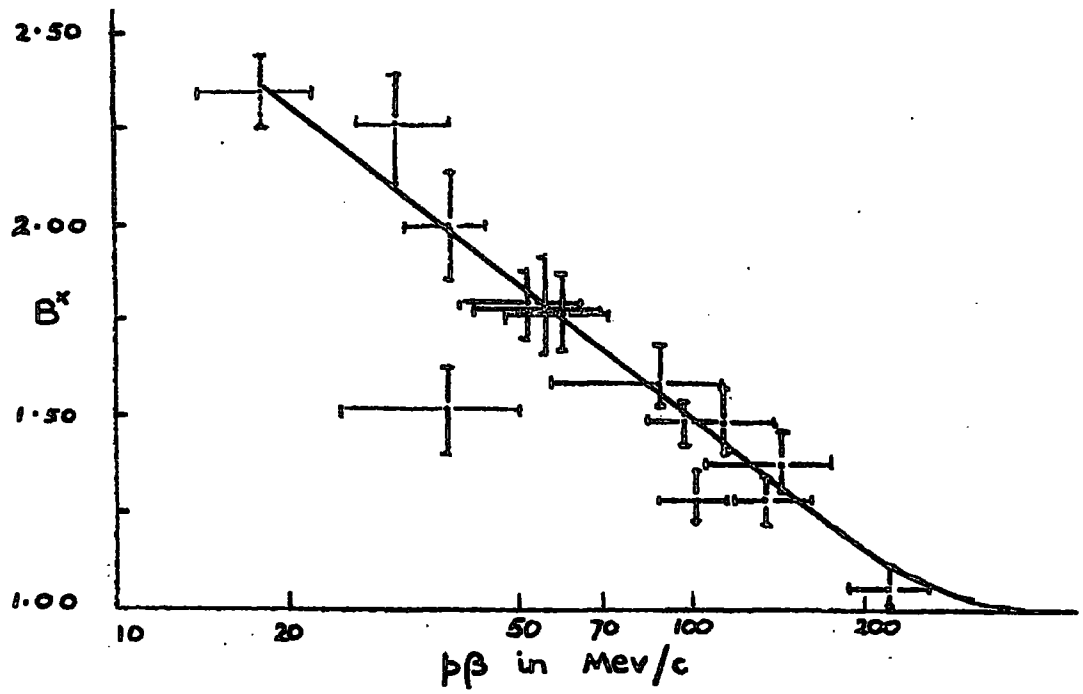

Fig 4B The relationship between corrected blob density and pβ for π^--mesons in G 5 emulsion.

Where K is approximately constant, with a value of 23.8 for a 100μ cell. The value increases slowly as the cell length increases.

For inclined tracks the true cell length will be t sec β, where t is the length of the cell measured in the plane of the emulsion and β the angle of dip. This correction has been incorporated in the work. It has been necessary to take measurements on steep tracks in this work because the object has been to separate π-mesons from other particles. Such measurements on even very steep tracks have often allowed the identification to be made with some certainty.

Generally the values of pβ are not more accurate than 15% because the observed tracks are relatively short.

2.4 Methods of identifying particles

During the early part of the experiment graphs relating to the blob density with range and the product pβ were constructed for protons and π-mesons. (Some deuterons may have been taken for protons). The protons and π-mesons were identified by their end-point characteristics or from a combination of pβ and range.

There is insufficient energy at 285 MeV to produce particles other than low energy mesons.

The maximum momentum which a proton can be given when struck by a beam particle is of the order of 800 MeV/c. This corresponds to a pβ value of ~530 MeV/c and a value of B^x of 1.63. Any track with a B^x less than this must be produced by a π-meson.

For a set of 125 consecutive stars, all prongs of $B^x > 1.63$ have been followed to their end, had the B^x at different ranges measured or had their $p\beta$ determined. 314 prongs have been identified.

Another set of 58 stars (chosen as likely to contain π-meson secondaries) has had all its 173 tracks fully identified.

Very steep tracks have been most carefully examined in order to make full use of the available information.

Short tracks of less than 100μ length have been taken as protons. Little error is introduced this way.

CHAPTER 3

THE ELASTIC INTERACTIONS OF 285 MEV Π-MESONS

3.1 Experimental Details

A stack of 60 pellicles of G5 emulsion, each 10 x 10 x 0.4 cm, was exposed to the beam of 285 MeV π^--mesons produced from the 660 MeV proton synchrotron at C.E.R.N., Geneva. Afterwards the pellicles were mounted on glass backs and processed by the temperature cycle method. The distortion was approximately 30μ.

The plates were examined by following tracks which were each picked up 1 cm from the edge of the stack at which the beam entered. A track was followed only if it made an angle of less than 3^0 with the main beam direction. This was to remove the possibility of following secondary mesons. Tracks were followed under a magnification of 45 x 15 x 1.5 until they interacted or travelled the maximum traverse of the stage which was 2.5 cm. All interactions of the meson, including scatterings through a horizontally projected angle greater than 3^0 were recorded. Spatial angles of scatter were found using the coordinate method.

Interactions were classified using the notation $(n_H + n_s)\pi$ where n_H and n_s are the numbers of heavily and lightly ionizing ($B^x \lesssim 1.6$) tracks which are generated. For example, elastic scatterings are classified as $(1+1)\pi$, disappearances as $(0 + 0)\pi$. Each event was checked by two observers to reduce the chance of missing tracks which were near the minimum of ionization or steep.

Only an approximate figure of about 10% was available as the percentage contamination of the beam by μ-mesons and electrons. An attempt to compute the proportion of μ-mesons in the beam from the beam layout lead to a figure of a few percent, (~3%). The proportion of electrons was estimated experimentally by finding the distribution of blob densities in 100 tracks, each 2.5 cm long, in the beam. At 285 MeV, an electron will ionize at the minimum, which is about 10% below the plateau value. No evidence for electrons was found.

No correction has been applied because of the above findings. It is usual to accept 5% as a working contamination for such a beam.

3.2 Interaction Length

A total length of 140.0 m of track was followed. 255 elastic events, having a horizontally projected angle greater or equal to 3°, and 370 inelastic interactions (all other events) were found. The inelastic events contain 42 disappearances. The mean free path for inelastic interaction is (37.9 ± 2.0)cm. In the group classified as being elastic scatterings of the π-meson, 8 events were identified, dynamically, as being collisions between the π^--meson and a free proton.

A calculation has shown that the scattering of Φ less than 5° results largely from Rutherford scattering in the Coulomb field rather than in the nuclear field of the nuclei. Consequently,

attention has been confined to those scatterings with ϕ greater or equal to 5° for which the measured mean free path is (77 ± 5.8)cm.

The values of the m.f.p. will be affected by the efficiency of the scanning. Stars of small size might well be missed. This can be tested by noting the measured frequency of a small sized event which occurs with a known cross-section. Such an example is the elastic scattering of π-mesons by the hydrogen in the emulsion which leads to events of the type $(1 + 1)\pi$. The elastic scattering occurs with a cross-section of 11 mb. This would lead to an expected number of 5 scatterings. In fact 8 have been identified. This observation together with the fact that a large number of disappearances have been found suggests that there has been a high efficiency of detection of small events.

Some of the $(0+1)\pi$ events may have been wrongly classified as elastic scatterings. Some of these may be inelastic interactions with neutron emission. In those stars where secondary mesons have been found, the forward-backward ratio for their emission is (0.74 ± 0.17). Assuming that all the 13 scatterings with backwardly scattered mesons are really inelastic interactions with neutron emission and also assuming that the F/B ratio of 0.74 is appropriate, then 9 inelastic scatterings are expected, classified as $(0 + 1)\pi$, in which the meson is scattered forwards. These 13 + 9 misclassified events would alter the mean free path for elastic scattering by 12% and the inelastic m.f.p. would be reduced by 5%. No corrections have been made as these represent upper limits.

3.3 Application of the Optical Model to the results

The Optical Model can supply various information about the nucleus. (see section 1.4). By considering equations 1.3.1 and 1.4.1 a relationship between λ, the inelastic interaction length, and K, the absorption coefficient, can be found. This is shown as curve A in figure 5. The correction for the reduced de Broglie wavelength and the coulomb attractive forces (as mentioned in 1.3) are shown as curves B and C respectively.

Using the observed value for λ of (37.9 ± 2)cm and curve B an absorption coefficient, K equal to $(1.5 \pm 0.15)10^{12}$ cm^{-1} is found. This corresponds to a m.f.p. for interaction within the nucleus, λ_n of $(6.7 \pm 0.7)10^{-13}$ cm and to an opacity of the nucleus of 66%. This mean free path is about 1.5 times the mean emulsion constituent radius.

Using the value of the absorption coefficient K, found above, the angular distribution for diffraction scattering can be computed from (1.3.3) for various assumed values of k_1, the change in wave number of the meson wave upon entering the nucleus. These distributions are shown in fig. 6 which also shows the Rutherford scattering. The appropriate value of k_1 has been found by integrating the curves from 8^o upwards to determine the mean free path for scattering through angles greater than 8^o. These values were compared with the observed value from whence $k_1 = (1.32 \pm 0.12)10^{12}$ cm^{-1}. The sign of

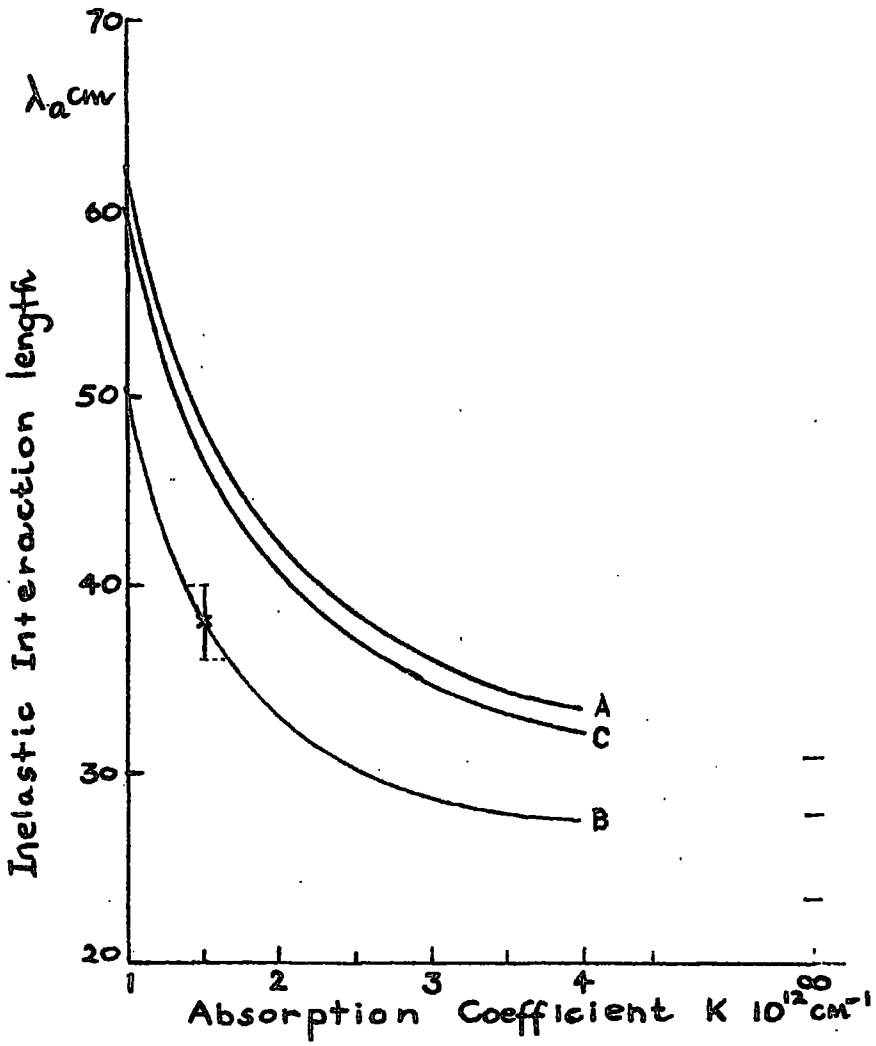

Fig 5 The variation of the inelastic interaction length with absorption coefficient.

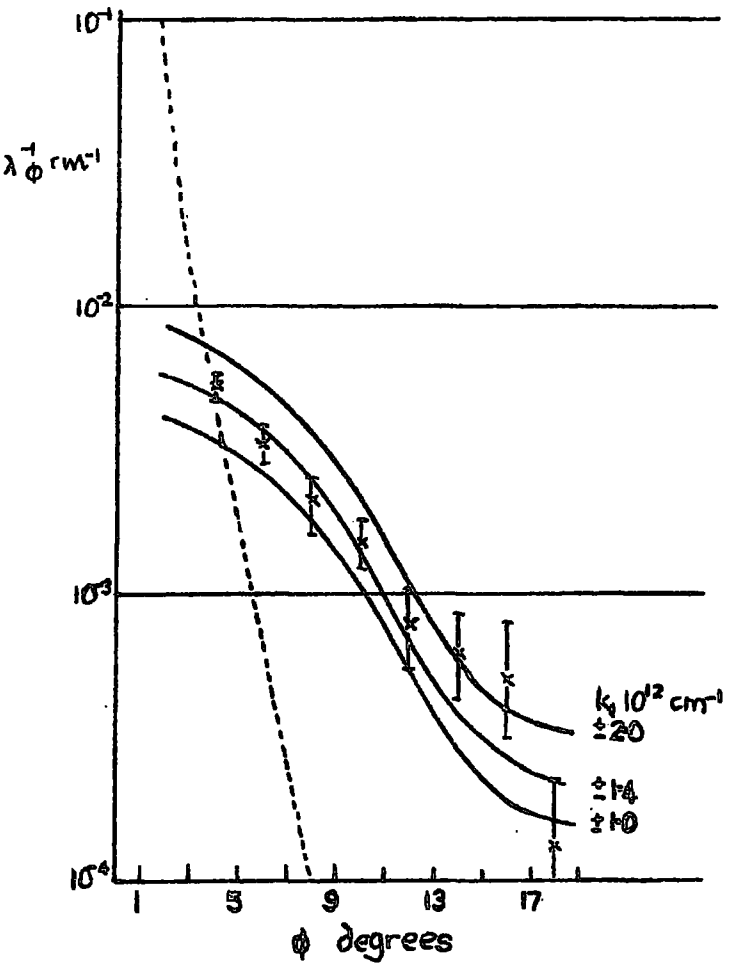

Fig 6 The distribution of projected angles of elastic scattering for π^--mesons in complex nuclei. The broken line is for Rutherford scattering.

k_1 is expected to be negative (Sternheimer, 1956).

The above results may be used in (1.3.7) and (1.3.8) to find the real and imaginary components of the nuclear potential, V_r and V_i. They are:

$$V_r = (25 \pm 1) \text{ MeV}$$

$$V_i = -(14 \pm 1.4) \text{ MeV}$$

If it is assumed that interaction in the nucleus takes place with scatterings on individual nucleons, then K will be determined by the cross-sections in hydrogen $\sigma_{\pi^- n}$ and $\sigma_{\pi^- p}$ which are equivalent to $\sigma_{\pi^+ p}$ and $\sigma_{\pi^- p}$. These cross-sections have been interpolated from Yuan (1956) and are (75 ± 5)mb and (32 ± 2)mb respectively. These values lead to a figure of $(5.2 \pm 0.3)10^{12}$ cm^{-1} for K.

If the interaction were due only to the absorption of the meson by a nucleon pair then use must be made of the cross-section for absorption of a π^--meson by deuterium. No data for this exists at 300 MeV but the results of Neganov and Parfenov (1958) suggest a $1/E^3$ dependence of the cross-section with kinetic energy, E. This leads to a value of (1 ± 0.1)mb at 300 MeV from which a value for K of $(0.50 \pm 0.05)10^{12}$ cm^{-1} is obtained. Consequently absorption of the meson wave corresponding to inelastic scattering should be predominant and the expected value of K is $(5.2 \pm 0.3)10^{12}$ cm^{-1} which is 3 to 4 times larger than the observed value.

Now the observed value of the absorption coefficient corresponds to a long mean free path inside the nucleus of about 1.5 times the nuclear radius. Most mesons, then, will make one collision only in passing through the nucleus. At this collision scattering or absorption occurs. The values of the observed probabilities of inelastic scattering and absorption can thus be taken to be the probabilities of these processes at the first collision. These are ~30% and ~70% respectively - i.e. absorption and not scattering is predominant. Adding the expected values of K(scattering) and K (absorption) in the proportions of these probabilities leads to an expected value of K of $(1.9 \pm 0.2)10^{12}$ cm^{-1}. This is in reasonable agreement with the observed value.

Table 1 shows the values of K found by other workers.

It is always possible to make the observed and calculated values of K agree by adjusting the size of the radial parameter r_o. If r_o is reduced to 1.12×10^{-13} cm then the experimental and theoretical values of K would agree at 9.3×10^{12} cm^{-1}. A large value of K, such as this, implies that the meson makes, on the average, about 5 collisions in the nucleus. This is not expected. It implies that the mesons should emerge from the nucleus with an energy of about 70 MeV, much lower than the average energy 107 MeV observed. The value of $r_o = 1.12 \times 10^{-13}$ cm is also outside the accepted range for this parameter.

TABLE 1

$\pi^{\pm}$	K.E of π MeV	Absorber	Observed cross-section σ, or mean free path λ	Probability of inelastic scattering P_s%	Geometrical cross-section or m.f.p.*	$K(10^{12}cm^{-1})$	Reference
π^+	282	(C $C\ell_2$ F_2)	(442 ± 31)mb	(44 ± 5)	469mb	(2.8 ± 0.5)	1
		C	(269 ± 26)mb	-	362mb	(2.6 ± 0.5)	
π^-	290	Cu	(918 ± 76)mb	-	915mb	(2.7 ± 0.8)	2
		Pb	(2313 ± 175)mb	-	2010mb	lower limit ~4	
π^-	300	NIFKI	(29.6 ± 1.6)cm	(32 ± 2)	25cm	(1.8 ± 0.2)	3
π^-	300	G5	(31.2 ± 4.3)cm/	(32 ± 4)	29.3cm	lower limit ~2	4
π^-	~300 (295)	G5	(37.2 ± 4.3)cm	30	29.3cm	(1.53 ± 0.15)	5

* With $r_o = 1.35 \times 10^{-13}$cm

/ Computed from area scanning data.

1. Meshkovskii and Shalamov, 1960

2. Ignatenko et al., 1957

3. Dulkova et al., 1956

4. Chemel, 1959

5. This work.

These results, leading to agreement between the expected and experimental values for K, suggest that the basis for calculating K is probably correct. i.e. the results are consistent with the inelastic interaction taking place by a single collision in which absorption and not scattering is the predominating feature. Consequently the cross-section for scattering of the meson by a single nucleon at ~300 MeV is reduced by a factor of ~3 within the nucleus.

CHAPTER 4

THE INELASTIC INTERACTIONS OF 285 MEV π^--MESONS

In the process of line scanning, 370 inelastic interactions were found. As a preliminary, the star sizes were determined together with the average number of black and grey tracks per star (n_B and n_G) and their forward to backward ratios of emission relative to the primary beam $\left((F/B)_B \text{ and } (F/B)_G\right)$.

A full analysis, using the techniques described in Chapter 2, was made on 125 interactions found successively during the scanning in which the identity, energy and spatial angle of emission of each secondary particle was determined. In 31 of these stars a pion secondary was observed. By examining those other stars which seemed likely to contain a meson secondary - i.e. largely those with grey or lightly ionizing secondary tracks - the number of stars with pion secondaries has been increased to 80.

These 80 events are classified as inelastic scatterings and the remaining 290 as absorptions. Charge exchange scatterings are grouped with the absorptive events but they are expected to be about 20% as frequent as the inelastic events. This means that they will form only 5% of the absorption events.

In the following sections the inelastic scatterings and absorption events are considered in some detail.

4.1 Inelastic scattering : Experimental results

When a π-meson collides with a stationary nucleon there is a unique relationship between the angle through which the pion is scattered and its energy. In the nucleus this unique relationship will not hold because, for instance, the target nucleons are moving. This means that for any given angle of scattering, θ there is a spread in the energies of the scattered pion.

In fig. 7 the mean energy, $\bar{E}_\pi$, for four angular intervals of scattering is shown together with similar data for inelastic scattering in carbon (Major 1963) and in NIKFI emulsion (Belovitskii 1959). Also shown, as the curve, is the unique relationship between θ and $\bar{E}_\pi$ for the collision of the pion with a stationary nucleon. The three sets of experimental data show a definite dependence of $\bar{E}_\pi$ upon θ and that this dependence is very similar to that found when a pion is scattered by a single, stationary nucleon. This suggests that the interaction involved in inelastic scattering at 300 MeV is one of scattering of the pion by a single nucleon in the nucleus. The differences, largely in the forward direction of scattering, might be explained, for example, by multiple scatterings of the pion or the inhibition of small energy transfers by the exclusion principle. These possibilities will be considered in section 4.3.

The angular distribution of the scattered pions is shown as a histogram in fig. 8. The dotted line represents an isotropic distribution of 80 events. The curves represent the angular

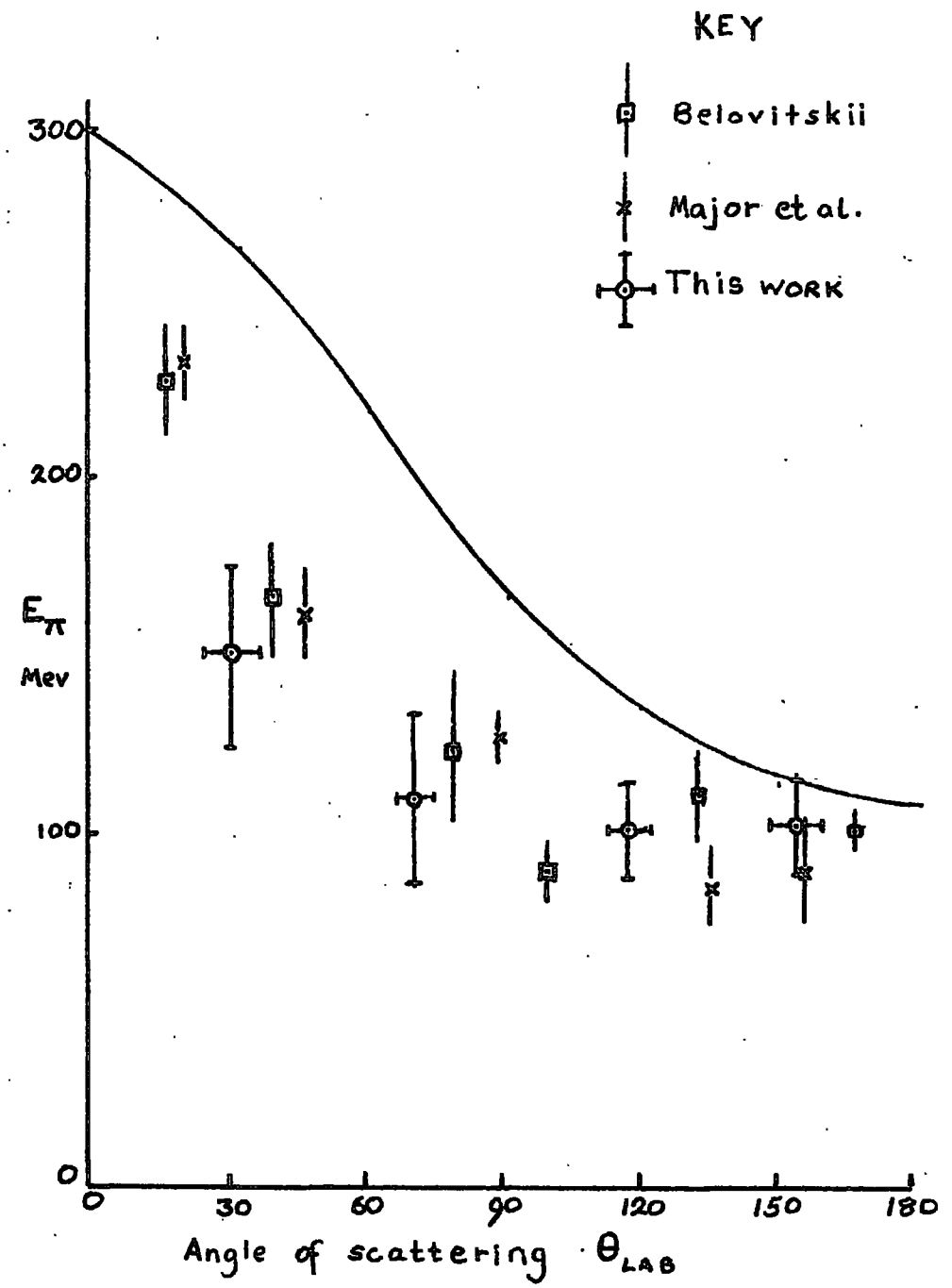

Fig 7 Mean energy of the scattered π^--meson against angle of scattering.

distributionfor the scattering of pions on stationary protons and neutrons, normalised on the total 80 events (curve A) and normalised on those pions which have been scattered backwards (curve B). The discrepencies are seen to be chiefly in the forward direction once again and might be explained by multiple collisions or by the exclusion principle. Similar experimental results have been found by other workers. These results are summarised in table 2 where the angular distribution is expressed as a forward to backward ratio of the emitted pions. The mean of the values is about unity.

Table 2

The forward to backward ratio for pions which have been scattered by a target.

$\pi^{\pm}$	Energy	Target	F/B	Reference
π^+	260 MeV	C	(1.29 ± 0.29)	Wang Kan-Chang 1959
π^+	300 MeV	NIKFI	(1.50 ± 0.33)	Belovitskii 1959
π^-	300 MeV	NIKFI	(1.19 ± 0.23)	Belovitskii 1959
π^-	300 MeV	G5	(0.84 ± 0.19)	Chemel (1961)
π^-	285 MeV	G5	(0.74 ± 0.17)	this work
π^-	285 MeV	(p,n)	2.8 ± 0.2	calculation

4.2 Inelastic Scattering : Discussion

It has been mentioned above that the results of fig. 7 are similar to those expected from a collision with a single, free nucleon. In order to establish a mode of interaction modifications

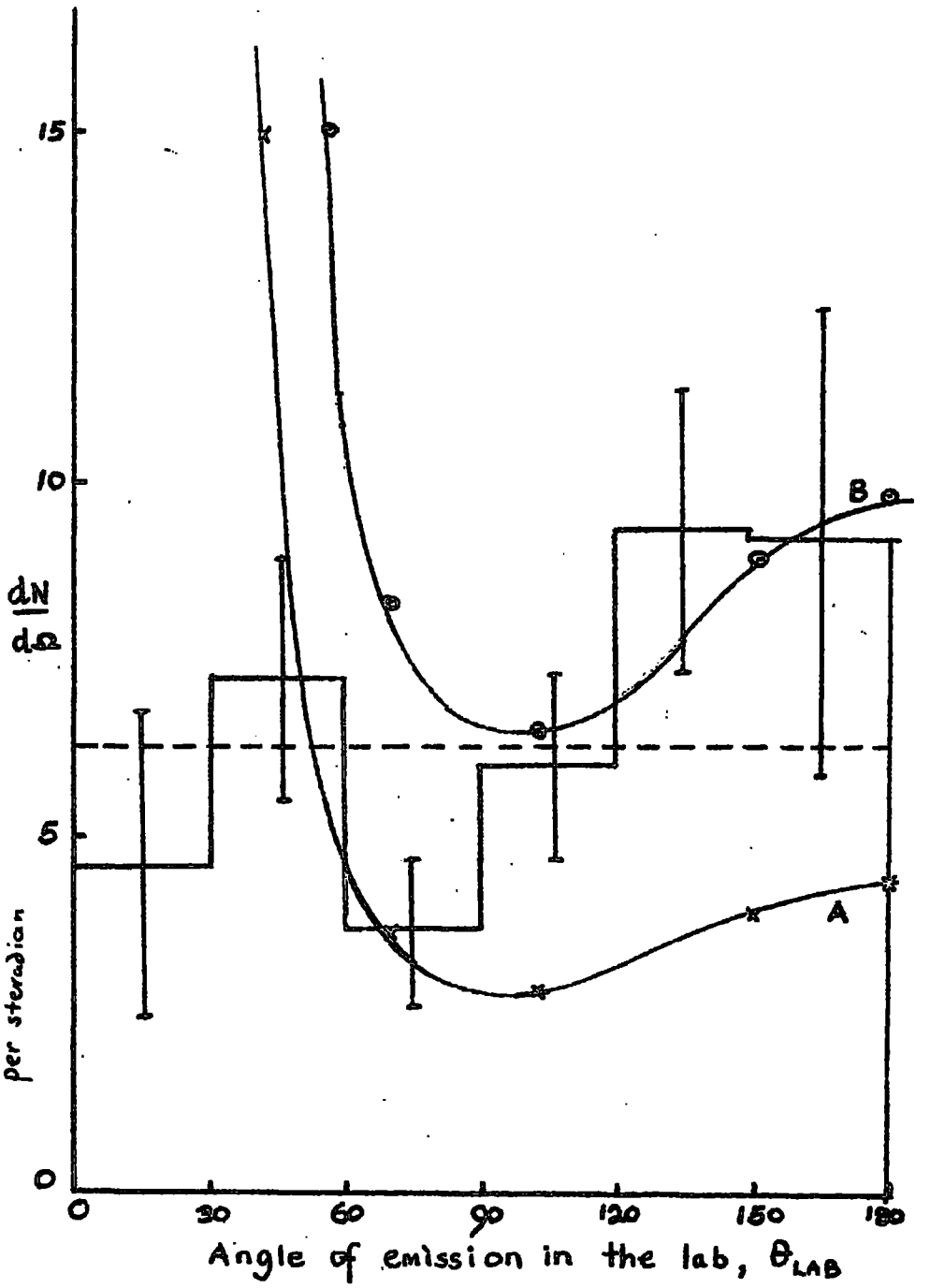

Fig 8 Angular distribution of inelastically scattered π^--mesons.

will be considered to scattering when this process occurs in the nucleus.

4.2.1 Multiple Collisions

An isotropic distribution for the scattered pions would be expected if many collisions occur between the pion and a moving nucleon. The mean energy, $\overline{E}_\pi$ should be much smaller for all angles than that represented by the curve of fig. 7 and there should be no correlation of $\overline{E}_\pi$ with θ.

This process could account for the observed F/B ratio for the pions but for neither their average energy nor the observed angular dependence on $\overline{E}_\pi$.

4.2.2 Motion of the nucleons

The nucleons of the nucleus are moving with a momentum of about 200 MeV/c. As a consequence of this, an approximate calculation shows that the angular distribution shown in fig. 8 curves A and B will be smeared by about 25° but nevertheless will still remain strongly peaked in the forward direction. Another calculation shows that the curve of fig. 7 will only be modified slightly.

Thus on average the motion of the struck nucleon will only make slight modifications to the results of a pion scattered by a stationary nucleon.

4.2.3 Effects of the exclusion principle

Small energy transfers from the pion to a target nucleon are inhibited by the exclusion principle. In general small energy transfers occur when the pion is scattered through a small angle. This means

that inhibition of small energy transfers is accompanied by inhibition of small angle scatterings, which occur in the forward direction. If the inhibition is severe, then the expected strongly forward to backward ratio of (2.8 ± 0.2), obtained by calculation, may be reduced to isotropy or even into backward peaking. The expected forward mean energy for the scattered pion will then be considerably reduced. The scattering through a large angle into the backward direction is usually accompanied by large energy transfers and so will be less inhibited. Fig. 7 clearly shows that the forward mean pion energy has been reduced whilst that in the backward direction is in good agreement with the expected energy if single collisions are the main process for interaction.

The near isotropy of the angular distribution of the pions is interpreted as a direct consequence of the exclusion principle. The small, forward angle scatterings have been severely inhibited.

Since the backward scattering of pions is less affected by the exclusion principle, nomralisation of the free nucleon angular distribution (fig. 8) has been made on the 46 scatterings in the backward direction. This is shown as curve B.

The area under curve B represents the cross-section for scattering of pions on free nucleons whereas the area under the histogram represents the observed cross-section, on bound nucleons. The ratio of the cross-sections is a measure of the effect of the exclusion principle and its value is (2.3 ± 0.4). This is a lower

limit since the effects of the exclusion principle in the backward direction has been ignored. Thus the cross-section for the scattering of a π^--meson by a free nucleon is reduced by a factor of 2.3 when the nucleon is bound in the nucleus.

A reduction factor of~3 was proposed at the end of Chapter 3 as a result of the analysis of the diffraction scattering and inelastic interaction by the Optical Model.

Reductions of this magnitude due to the exclusion principle cannot be achieved with the Fermi distribution of momenta for nucleons in the nucleus where the maximum momentum is about 220 MeV/c. However, the experimentally determined distribution of momenta (Garron et al. 1961) contains components with a momentum as high as 350 MeV/c and with such distributions reductions in cross-section by a factor of 3 can be realised. Preliminary calculations have been made by Apostolakis et al. (1963) using the distribution of Garron et al. If the distribution extends to about 450 MeV/c, the effect of the exclusion principle on 300 MeV pions is to reduce the scattering cross-section by a factor of 3 and the scattered pions have a F/B ratio of unity, in agreement with the present results.

4.3 Analysis of the Inelastic Interaction

4.3.1 Inelastic Scattering

The scheme proposed is that the incident pion makes a single collision with a nucleon. From the relative cross-sections for the interaction of a 300 MeV π^--meson with protons and neutrons,

90% of the scatterings (excluding charge exchange) occur with a neutron, and the pion emerges without further encounter. The neutron, which may be quite energetic, will probably interact with a nucleon before emerging from the nucleus. Again, from relative cross-sections, it is expected that the neutron will collide with a proton. The struck proton will, on average, recoil with half the energy of the neutron which struck it. This recoiling proton will give rise to a grey prong, which, in general, should be in the forward direction relative to the incident meson. Evaporation particles will then be ejected isotropically by the nucleus; these are the black prongs of stars. This is confirmed by the results of this experiment, as shown in table 3.

Table 3

The mean energies and forward to backward ratios for secondary π^--mesons, grey prongs and black prongs from inelastic scatterings.

	Secondary π^--mesons		Secondary grey prongs		Secondary black prongs	
	$\bar{E}_\pi$ MeV	$(F/B)_\pi$	$\bar{E}_G$ MeV	$(F/B)_G$	$\bar{E}_B$ MeV	$(F/B)_B$
All π secondaries	(107±12)	(0.74±0.17)	(58±11)	(5.8±3.1)	(9.8±0.9)	(1.3±0.2)
$E_\pi > 85$ MeV	(164±26)	(1.1±0.35)	(45±16)	(7 ± 7)	(9.5±1)	(1.36±0.37)
$E_\pi < 85$ MeV	(50±8)	(0.46±0.16)	(63±14)	(5.3±3.3)	(10 ±1)	(1.3±0.3)

After the collision of primary pion with the neutron, the neutron strikes a proton which loses about 30 MeV excitation energy, Pugh and Riley (1961), before emerging as a grey prong. It is possible to

estimate the energy of the initial neutron E_n as $\overline{E}_n = 2(\overline{E}_G + 30)$ MeV. In this case $\overline{E}_n = (176 \pm 22)$ MeV, which together with the value of $\overline{E}_\pi$ emitted leads to a value of 283 MeV.

A similar energy balance can be made with the data of table 3 for the two cases when the value of the emerging pion is either greater or less than 85 MeV, the energy which divides the mesons into two groups of 40 each. These results are summarised in table 4. The total energy should be 285 MeV and the results are in good agreement with this.

Table 4

The energies involved in an energy balance performed on inelastic scatterings

Energies in MeV	$\overline{E}_\pi$	$\overline{E}_n$	$\overline{E}_{total}$	Primary Energy
All π secondaries	(107 ± 12)	(176 ± 22)	(283 ± 25)	285
$E_\pi > 85$ MeV	(164 ± 26)	(150 ± 32)	(314 ± 41)	
$E_\pi < 85$ MeV	(50 ± 8)	(186 ± 28)	(236 ± 29)	

On summarising the above results, it is seen that the inelastic scattering of pions in nuclei is consistent with a single scattering of a pion on a moving nucleon in the nucleus. The recoiling nucleon, in general, has an observed probability of about 50% of interacting with a second nucleon before emerging from the nucleus.

4.3.2 Absorption of the pion

It will be assumed that the pion is absorbed by a proton-neutron pair to form a pair of neutrons.

The effect of the exclusion principle is to make inelastic scattering of pions proceed largely through a single scattering of the pion by a nucleon, which implies a long mean free path in nuclear matter for the π-meson. Hence it is unlikely that the absorption process will be preceded by a scattering. The two neutrons produced by the absorption will share the total energy of the pion. A calculation has been made which shows that the neutron recoiling in the forward direction with an energy range of 227 to 303 MeV whereas for that in the backward direction the energy range is between 111 to 227 MeV. The average energies of recoil are about 265 MeV and 169 MeV for the forward and backwards recoiling neutrons. The forward to backward ratio of the neutrons is expected to be 1.94 . Since the neutron energies are of the same order as the neutron energies resulting from the inelastic scattering of the pion, and since two neutrons are produced in this case, it is expected that absorption will be accompanied by twice as many grey prongs as inelastic scatterings. The mean energy of the grey secondaries $\bar{E}_G$, should be the same in the two cases.

The forward to backward ratio will be modified because the backward recoiling neutron, of lower average energy, has a larger cross-section for interaction with protons than the higher energy forward scattered neutron. This effect is expected to modify the

$(F/B)_G$ ratio for grey tracks to a value of 1.4. The evaporation prongs should be black, distributed isotropically and of the same mean energy as the evaporation prongs from inelastic scatterings.

Table 5 gives the data for the absorption events and average prong sizes for the inelastic scatterings. The results here should be compared with those in table 3.

Table 5

The mean energies and forward to backward ratios for grey and black secondary tracks from absorptive events. The mean grey and black star sizes are given for absorptive events and inelastic scatterings

Absorptive events

$\bar{E}_G$	$(F/B)_G$	$\bar{E}_B$	$(F/B)_B$	$\bar{n}_G$	$\bar{n}_B$
(64±11)	(1.2±0.2)	(9.5±0.7)	(1.14±0.09)	(0.40±0.004)	(2.24±0.14)

Inelastic scatterings

$\bar{n}_G$	$\bar{n}_B$
(0.34±0.07)	(1.5±0.25)

The forward to backward ratios for grey and black prongs and their energies are consistent with the predicted values but the number of grey prongs is not twice as large as the number of inelastic grey prongs.

From the average value of the grey prongs the expected energy of the pair of absorbing neutrons should be (376 ± 44) MeV. This should be the same as the total pionenergy of 422 MeV. Thus there is good agreement on this energy balance.

If the incident meson had been scattered once before absorption, the pion at absorption would have on the average a kinetic energy of 107 MeV. Hence the energy shared by the neutron pair would be about 250 MeV. Since this does not agree with the 'observed' value, it is concluded that absorption of a pion by a pair of nucleons is not preceded by a scattering.

The star size distributions for heavy secondaries from inelastic scatterings and absorptive events is presented in table 6.

Table 6

Star size distribution for inelastic scatterings and absorptive events

No. of heavy secondary prongs	0	1	2	3	4	5	6	7	8
No. in inelastic events	6	29	25	13	6	1	-	-	-
No. in absorptive events	42	47	44	66	44	31	10	5	1

4.4 Conclusions

At 285 MeV the inelastic scattering and absorption of a π^--meson in the nucleus is readily interpreted by a single collision only of the pion with one nucleon in the former case and two in the latter case. From the known cross-sections for scattering in hydrogen

(see Chapter 3) the probability that more than one collision should take place is quite ~~small~~ high. It would appear that the probability of scattering in the nucleus is reduced so that only a single scattering occurs. In chapter 3, it was concluded from an Optical Model analysis that the cross-section is reduced by a factor of 3. A possible mechanism is the exclusion principle. In this chapter the almost isotropic angular distribution of the inelastically scattered pions is accounted for. By making the reasonable assumption that the backward scattered mesons are not inhibited by the exclusion principle very much, the reduction factor for the cross-section is 2.3. The forward scattering is most strongly inhibited because this is the region where small energy transfers are forbidden. Consequently there is good agreement between the expected mean pion energy and observed values.

Such pronounced effects through the exclusion principle are not possible with a Fermi distribution of momenta. However, the recently measured nuclear momentum distribution is such that preliminary calculations show that large inhibitive effects may occur.

Experiments are being conducted in these laboratories to test the validity of such calculations.

ACKNOWLEDGMENTS

The author wishes to thank Professor G.D. Rochester for accepting him into his research laboratories. For help with the work on inelastic scatterings and many useful discussions Mr. P.J. Finney is thanked. But above all the author remains indebted to Dr. J.V. Major for truely unfailing help and encouragement at all times. The D.S.I.R. are thanked for a maintenance grant.

REFERENCES

1. Apostolakis, A.J., Major, J.V., Welton, M.G.E., 1963, Priv. Com.
2. Belovitskii, G.E., 1959, Soviet Physics, 8, 581.
3. Chemel, B., 1961, Ann. de Physique, 6, May.
4. Chemel, B., 1959, C.R. Acad. Sci., Paris, 249, 1625.
5. Cladis, J.B., Hess, W.N., and Moyer, B.J., 1952, Phys. Rev., 87, 425.
6. Cronin, J.W., Cool, R. and Abashian, A., 1957, Phys. Rev., 107, 1121.
7. Dowell, J.D., Frisken, W.R., Martelli, G. and Musgrave, B., 1960, Proc. Phys. Soc., Lond., 75, 24.
8. Dulkova, L.S., Romanova, T.A., Sokolova, I.B., Sukhov, L.V., Tolstov, K.D., and Shafronova, M.G., 1956, Dokl. Akad. Nauk, SSSR, 107, 43.
9. Fay, H., Gottstein, K., Hain, K., 1954, Supp. Nuovo Cimento, No. 2.
10. Fernback, S., Serber, R., Taylor, T.B., 1949, Phys. Rev., 75, 1352.
11. Feshback, H. and Weiskopf, V.F., 1949, Phys. Rev., 76, 1550.
12. Finney, P.J., Major, J.V., Parkhouse, P.G.J.T., 1962, Phil. Mag., 7, 237.
13. Garron, J.P., Jacmart, J.C., Riou, M., and Ruhla, C., Proceedings of Rutherford International Conference, 1961, p. 201.

14. Hodgson, P.E., 1952, Brit. J. App. Physics, 3, 11.

15. Hofstadter, R., 1956, Rev. Mod. Phys., 28, 214.

16. Ignatenko, A.E. and Mukhin, A.I., Ozerov, E.B., and Pontecorvo, B.M., 1957, Sov. Physics, 4, 351.

17. Major, J.V., Priv. Comm., 1963.

18. Meshkovskii, A.G., and Shalamov, Y.Y ., 1960, Soviet Physics, 10, 697.

19. Neganov, B.S., and Parfenov, L.B., 1958, Soviet Physics, 7, 528.

20. Perkins, D.H. and Daniel, R.R., 1954, Proc. Roy. Soc., A221, 351.

21. Perkins, D.H. and Fowler, P.H., 1958, Priv. Comm.

22. Pugh, H.G., and Riley, K.F., Proceedings of the Rutherford International Conference, 1961, p. 195.

23. Sternheimer, R.M., 1956, Phys. Rev., 101, 384.

24. Viriasov, N.M. and Pisareva, L.P., 1958, Inst. and Exp. Techniques, 2, March-April, 1958.

25. Wang Kan-Chang, Wang Tso-Tsiang, Ding Da-Tsao, Dubrovskii, L.N., Kladnitskii, E.N., Solovev, M.I., 1959, Soviety Physics, 8, 625.

26. Yuan, L.C.L., 1956, Cern Symposium, 2, 195.